Brownian Ratchets and the Photoalignment of Liquid Crystals

P. Palffy-Muhoray[a], T. Kosa[a], and Weinan E[b]
[a] Liquid Crystal Institute, Kent State University, Kent, OH 44242
[b] Mathematics Department, Princeton University, Princeton, NJ 08544

Received on 11 December, 2001

Molecular motors play key roles in areas ranging from biological transport to emerging nanotechnology. They produce current as a result of transfer of energy but not of momentum from a source; many molecular motor scenarios are based on the translational Brownian ratchet mechanism. Here we consider the mechanism of photoalignment of liquid crystals both in the bulk and at the surface by a photosensitive alignment layer. We show that the photoalignment is due to an orientational ratchet mechanism, where the azo-dye molecules, functionalized into a polymer alignment layer, when irradiated by polarized light act as the rotors of Brownian motors which reorient the bulk liquid crystal against an elastic restoring torque. Results of this photoalignment experiment can be obtained directly from a remote experiment set up at the Liquid Crystal Institute, via the WWW. In addition to experimental results, we present a detailed Fokker-Planck description of this system. We discuss the implementation and the results of numerical simulations, and compare these with the experimentally observed dynamics.

I Introduction

It is well known that light can exert a force on matter; radiation pressure on a reflecting metal surface, or a black absorbing surface are well known examples. It is perhaps less well known that light falling from vacuum on a dielectric interface exerts a force which attracts the interface towards the source of light [1]. In 1936, R.A. Beth showed that light can also exert a torque [2]; in his example, the torque, along the wave vector of light, was due to the transfer of intrinsic (spin) angular momentum from the radiation field to the material. In 1969, A. Saupe showed that light can also exert a torque, perpendicular to the wave vector, on liquid crystals [3]; this effect has subsequently been rediscovered by others [4-7] and has been the subject of considerable attention. In Saupe's experiment, the torque is due to the transfer of extrinsic (orbital) angular momentum from the radiation field to the material [8].

In 1990, Janossy showed that by adding a small amount of dichroic dye to the liquid crystal, the threshold intensity for the light induced reorientation is reduced by some two orders or magnitute [9][10]. Since in this case the transfer of extrinsic angular momentum from light is also reduced by some two orders of magnitude while the elastic restoring torques remain unaltered, it is clear that the torque felt by the liquid crystal cannot originate in angular momentum transfer. Understanding the details of angular momentum balance in this system posed an interesting and challenging problem. We have suggested that this 'rotation without torque' is an orientational version of the translational ratchet mechanism, capable of producing 'motion without force', proposed by Astumian [11] and Prost [12], and that the torque is carried from the cell walls by viscous shear to the dye molecules, which act as rotors of a Brownian motor [8]. Subsequently, this model has been significantly expanded [13,14].

In this paper, we argue that photoalignment by dye doped photosensitive alignment layers can also be due to the ratchet mechanism, where the dichroic dye molecules in the alignment layer act as rotors of Brownian motors.

I.1. Biological transport

It is interesting to explore parallels in the understanding of angular momentum balance in the photoalignment of liquid crystals, and of the mechanism of transport in biological systems. Essentially all living organisms (the eukaryotic cells of yeasts, plants, animals) contain 'motor proteins'. Two well known examples are kinesins and myosins. Kinesin has two active heads, it hydrolyzes ATP, and moves along processively along mictotubules.

Myosin also has two active heads, it also hydrolyzes ATP, and it moves processively along actin fibers. Although myosin is involved in a great variety of cell functions, it is perhaps best known for its role in muscle

tissue. The actin fibers in muscle are connected to Z-membranes forming the end of sarcomeres; the motion of the myosin heads on the actin fibers results in tension of the myosin strands, contraction of the sarcomeres, and of the muscle fiber [15]. The myosin fibers are approximately 15μ m long, exert a force of ~ 5 pN per attached head, the step-size is 5.5 nm and there is one step/ATP-ase reaction.

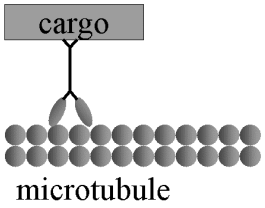

Figure 1. Schematic of kinesin carrying cargo along a microtube.

The mechanisms responsible for the transport of both kinesin and actin has been the subject of considerable discussion in the literature. The conventional view has been that myosin transport takes place via a 'lever-arm swinging' model, while actin transport takes place via 'hand-over-hand' motion [16].

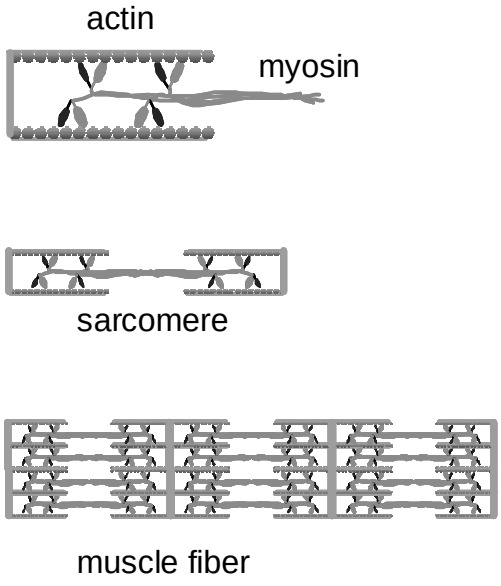

Figure 2. Schematic of myosin movement resulting in muscle contraction.

Recent experimental results have however cast doubt on the validity of these models. Ishii and Yanagida showed [17] that processive transport can be observed in myosin subfragments which are without the full mechanical 'lever-arm' component, indicating that the 'lever-arm' model cannot adequately explain the mechanism of the observed motion. Similarly, Okada and Hirokawa developed a mutant superfamily of one-headed kinesin, also capable of processive transport [18]. Their result suggested that the 'hand-over-hand' motion cannot adequately explain the mechanism of the observed motion. The conventional mechanical models thus apparently failed to explain the details of the observed processive transport.

It has now been proposed that both in the case of actin and of myosin, the mechanism for the observed 'motion without force' is the biased Brownian ratchet [19,20]; that is, essentially the same mechanism which is responsible for the anomalous threshold reduction in the Janossy effect, and, as we argue below, for photoalignment by dyed photosensitive alignment layers.

I.2 Motors and diffusive transport

In view of considerable recent discussion of molecular motors in the literature, it is interesting to inquire into the definition of a motor. We note that even conventional motors have the feature that they give rise to 'motion without force'. For example, in the road-car system, the car typically moves, not as a results of an externally applied force, but because the motor of the car causes one part of the system (the road) to exert a force on the other (the car) without any momentum transfer from outside the system. A working definition of motor may therefore be: *that wich causes motion in a system without momentum transfer from the outside, or, alternately, a machine that uses energy but not momentum to drive a current.*

Diffusive transport is the name given to model processes [21] which can drive a current of particles against an opposing viscous force. Unlike in conventional motors, intertia does not play a role. One early example of diffusive transport is the beautiful model proposed by R. Landauer [23], which has become known as Landauer's Blowtorch. Here particles experience a spatially periodic symmetric sinusoidal potential as well as a periodic temperature field, as shown in Fig. 3.

Since the temperature is shifted relative to the potential, particles near the left side of the valleys are at a higher temperature than those near the right; consequently they are more likely to be thermally excited over the potential barrier and diffuse to the left. The heat source in this arrangement therefore drives a steady current of particles against an opposing viscous force; the current flows without momentum transfer from the outside.

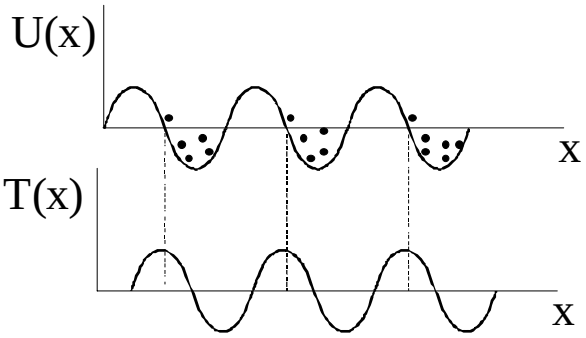

Figure 3. Landauers's Blow torch. Particles experience a static sinusoidal temperature field: the temperature is shifted $\lambda/4$ relative to the potential.

A schematic of the translational ratchet of Astumian [11] and Prost [12] is shown in Fig. 4.

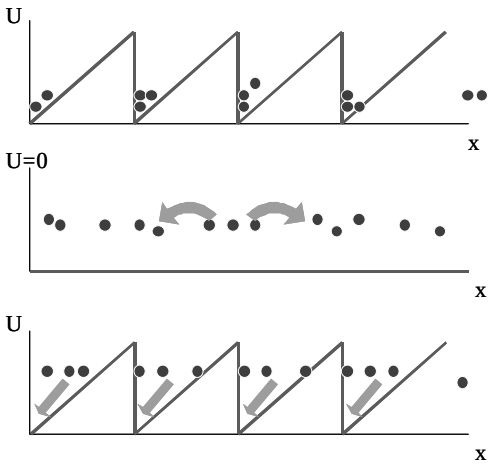

Figure 4. Schematic of the translational ratchet.

When the asymmetric potential is turned OFF, particles diffuse evenly in both left and right directions, and the net current is zero. When the potential is turned ON, the particles undergo directed diffusion under the influence of the potential, resulting in a net current to the left. A salient feature of the ratchet is a spatially periodic asymmetric potential which is periodic in time. The process is diffusive rather than inertial; the potential drives a current against an opposing viscous force. Turning the potential ON and OFF requires a transfer of energy, but not of momentum.

We now consider the Janossy effect (bulk photoalignment) and a photoinduced twist experiment in more detail, and argue that the key underlying process is an orientational ratchet mechanism.

II Liquid crystals

Liquid crystals are anisotropic fluids, characterized by orientational order of the constituent molecules. They are responsive 'soft' materials, since their inherent anisotropy provides a mechanism of coupling to fields, and their fluidity allows a large response.

Molecules of nematic liquid crystals prefer to be parallel; the direction of average orientation of the molecular symmetry axes is described by the unit vector director field. Nematics with positive dielectric anisotropy also prefer to align with an applied electric field; this effect plays a key role in liquid crystal displays. Molecular anisotropy also results in direction dependent surface interactions.

The free energy density, in the one elastic constant approximation, is given by [22]

$$F = \int \left\{ \frac{1}{2} K[(\nabla \cdot \hat{\mathbf{n}})^2 + (\nabla \times \hat{\mathbf{n}})^2] - \mathbf{\Delta}\varepsilon(\hat{\mathbf{n}} \cdot \mathbf{E})^2 \mathbf{dV} - \int \mathbf{W}(\hat{\mathbf{N}} \cdot \hat{\mathbf{n}})^2 \mathbf{dA} \right. \tag{1}$$

where K is an elastic constant, the dyad $\Delta\varepsilon\hat{\mathbf{n}}\hat{\mathbf{n}}$ is the anisotropic part of the dielectric tensor, $\mathbf{E}$ is the applied electric field, W is an anchoring strength and $\hat{\mathbf{N}}$ is the easy axis of alignment at the surface. In a sample of linear dimension R, the first term on the r.h.s. describing the energy cost of a non-uniform director field, is proportional to R, while the last term describing surface interactions is proportional to R^2. Consequently, in large samples ($R > K/W$), in the absence of fields, surface interactions dominate and determine the orientation. From Eq. (1), the torque per volume due to a static electric field is given by

$$\mathbf{\Gamma_{DC}} = \mathbf{\Delta}\varepsilon(\hat{\mathbf{n}} \cdot \mathbf{E})\hat{\mathbf{n}} \times \mathbf{E} = \mathbf{D} \times \mathbf{E} \tag{2}$$

When the director is parallel to the electric field, the torque vanishes.

If light is propagating in the liquid crystal, the torque density due to momentum transfer from light is the anisotropic part of the Maxwell stress tensor; this gives the direct optical torque

$$\mathbf{\Gamma_{OPT}} = \mathbf{D} \times \mathbf{E} \tag{3}$$

whose form is the same as in the static case.

II.1 Experimental observations

II.1.1 Optical reorientation in the bulk

The optical Fréedericksz transition. If plane polarized light is normally incident on a nematic cell where anchoring conditions are such that the director is normal to the cell walls, then, above a threshold intensity, the director tends to align along the electric field; that is, along the direction of polarization of the light. This is the optical Fréedericksz transition. A schematic is shown in Fig. 5. Due to anisotropy, **D** is not parallel to **E**, and the ray is deflected. Angular momentum is transferred from the light to the liquid crystal.

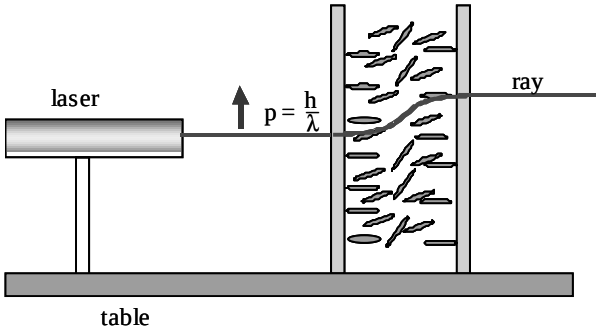

Figure 5. Schematic of the optical Fréedericksz transition.

The optical torque $\mathbf{\Gamma_{OPT}}$ is balanced by the elastic torque

$$\mathbf{\Gamma_{ELAST}} = K\hat{\mathbf{n}} \times \nabla^2 \hat{\mathbf{n}} \qquad (4)$$

in good agreement with experimental observations [24].

The Janossy Effect. In 1990, Janossy showed that if a small amount ($< 1\%$) of a dichroic dye is dissolved in the liquid crystal, the threshold intensity for the optical Fréedericksz transition can be reduced by up to two orders of magnitude [9]. The anomalous reduction of the threshold intensity is the Janossy effect. In the Janossy effect, the elastic torque remains essentially the same as in the pure material, since the elastic constant is not affected significantly by the presence of the small amount of dye [10], however, since the threshold intensity is reduced by some two orders of magnitude, the direct optical torque is correspondingly reduced. Since, as pointed out by Janossy [10], the direct optical torque is not sufficient to overcome the elastic torque, a different source of torque must exist.

II.1.2 Optical alignment at surfaces

Photoalignment.

Since surface interactions often determine the orientation of the director in the bulk, surface alignment is of great practical importance. In most liquid crystal displays, thin mechanically buffed polymer layers establish surface alignment of the director. Because of its potential for display and optical memory applications, the photoalignment of liquid crystals by photosensitive alignment layers generated a great deal of interest. One irreversible scheme uses polarized light to achieve direction-selective cross-linking [25,26] or breaking of polymer chains [27]. A reversible scheme uses a photosensitive alignment layer where dye molecules are either covalently attached to the substrate surface [28] or incorporated into a polymer matrix [29]. Here polarized illumination alters the orientation of the chromophores, which results in the change of the direction of the easy axis. This latter scheme shows considerable potential for applications [30], the photoinduced twist experiment discussed below makes use of it.

Azo dyes

Azo dyes are compounds containing -N=N- (azo) groups which are linked to various organic groups (substituents) through sp^2 hybridized carbon atoms [31]. With respect to both production and variety, azo dyes are by far the largest group of commercial colorants.

Due to the presence of the lone-pair electrons on the nitrogens, the azo bond, although planar, is not linear. There are two stereo isomers of azo compounds, depending on the relative position of the lone-pairs and substituents as shown in Fig. 6. Interestingly, although azo dyes were commercially produced as early as 1861, the *trans-cis* isomerization was discovered by G.S. Hartly only in 1937.

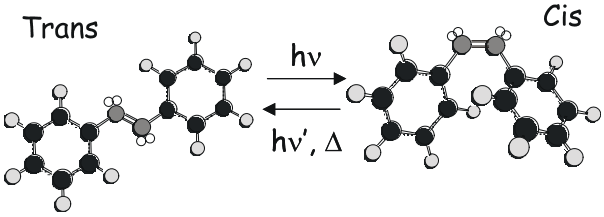

Figure 6. Trans- and cis- isomers of azobenzene. (The empty circles on the doubly bonded nitrogens indicate the lone-pairs electrons.

The elongated *trans*-isomer is thermodynamically stable, while the higher energy *cis*-isomer is metastable. The lowest energy optical excitation of azobenzene derivatives promotes non-bonding lone-pair electrons to anti-bonding π-like molecular orbitals, and is designated as (n, π^*) transition. The next higher energy excitation induces a (π, π^*) transition. Following the excitation, a transition between the two isomeric forms is possible. In general, there are two pathways available for the isomerization; rotation and inversion. Theoretical calculations predict that whether the isomerization takes place through the rotation or inversion

mechanism is greatly influenced by the nature of the substituent groups and by the excitation energy. Recent results of femtosecond spectroscopic measurements support the idea that (n, π^*) excitation of azobenzene leads to isomerization via inversion at one of the nitrogen atoms [32].

Due to the nature of the process, there are three properties that change upon isomerization: absorption, dipole moment and geometric dimension. These light induced changes lend azobenzene containing materials great potential in applications requiring photoresponsivity. Possible applications range from image and information storage to biological applications such as photoregulation of enzyme activity.

When a small amount of dye with elongated molecular shape is dissolved in a liquid crystal, the dye molecules tend to align parallel to the nematic director. By changing the orientation of the director, say, by applying an external electric field, the orientation of the dye molecules can be changed as well. This so called 'guest-host' effect has been utilized for display applications prior to the invention of the twisted nematic display [33].

With the discovery of the photoalignment method using azo dye-polymer systems[29], azo dyes became subjects of renewed scientific interest in the liquid crystal field.

III Photoinduced twist experiment

In the photoinduced twist experiment, a nematic cell with one mechanically buffed and one photosensitive alignment layer is irradiated with polarized light. Although the polarization is along the initially uniform director field, which is parallel to the buffing direction, the director field develops a photoinduced twist deformation [13].

The sample cells used in the experiment consist of two glass plates, separated by 20μ m spacers, and containing the liquid crystal 5CB between the plates. One plate was coated with a mechanically buffed polyimide layer which is expected to give strong planar anchoring. The other plate was coated with a 300Å thick photosensitive layer of PMMA into which the azo-dye Disperse Red 1 has been functionalized. The chemical structure of the photosensitive alignment layer is shown in Fig. 7.

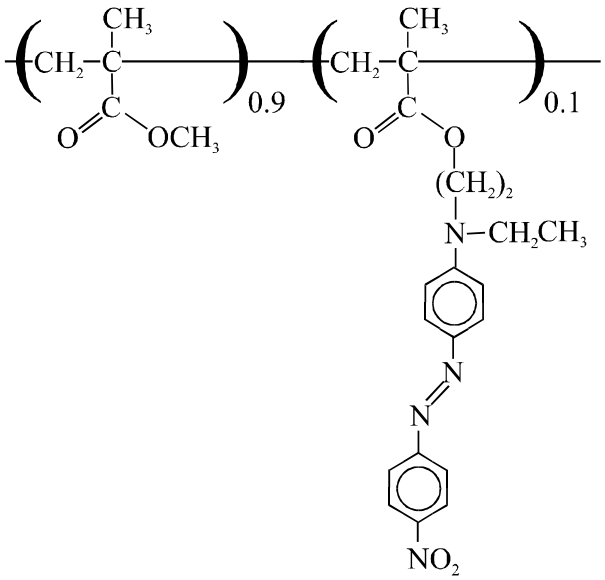

Figure 7. Chemical structure of the PMMA layer with the functionalized DR1 dye.

A schematic of the photoinduced twist experiment is show in Fig. 8. If there is no light incident on the photosensitive alignment layer, the alignment of the director in the cell is everywhere parallel to the buffing direction of the strongly anchoring mechanically buffed polyimide layer. When the cell is irradiated by plane polarized light at $\lambda = 514$ nm and at 20 mW of power from a CW Ar+ laser, with polarization parallel to the director, a twist deformation develops in the cell as shown in Fig. 8.

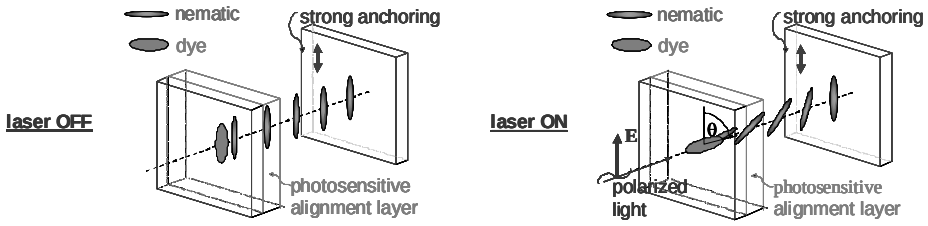

Figure 8. Schematic of the photoindicated twist experiment.

To measure the twist, a pump-probe arrangement was implemented; a He-Ne laser illuminating the sample between crossed polarizers was used as the probe. The experimental setup is shown in Fig. 9.

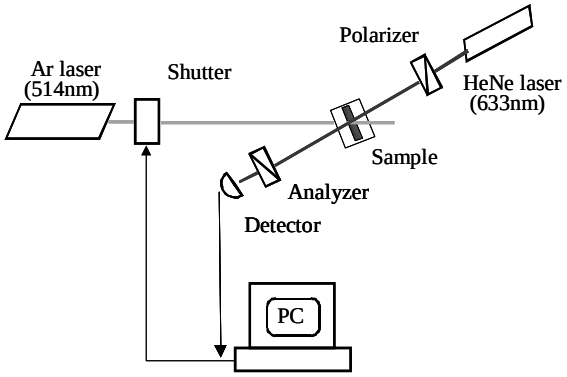

Figure 9. Schematic of the experimental setup.

When the cell is in the uniform planar state, the detector receives no signal, since the polarizer and analyzer are crossed. As the photoinduced twist develops under the influence of the pump beam, the transmitted intensity increases; the transmited intensity thus gives a measure of the twist in the cell.

III.1 Remote experiment on the Web

Equipment has been set up at the Liquid Crystal Institute at Kent State University which allows the photoinduced twist experiment to be carried out remotely, via the World Wide Web. Any user with Internet access and a Web browser can access the experiment at http://experiment.lci.kent.edu. In addition to obtaining access to background material describing the experiment and the equipment, remote users can control, in real time, the shutter, the pump polarization and the pump intensity. They can also obtain the signal from the detector as well as real video images of the experiment. A typical frame, showing the user interface, detector signal as function of time and video frame of the equipment is shown in Fig. 10.

The data shown in Fig. 11. is the intensity at the detector, in response to pump beam turned on at $t = 0$, with polarization parallel to the mechanical buffing direction on the back plate. The pump beam was shut off at $t = 110$ s.

III.2 Experimental results and discussion

Without photoexcitation, the cell adopts the uniform planar state, with the director everywhere parallel to the buffing direction of the mechanically buffed polyimide layer. As the plane polarized pump beam, with polarization parallel to the buffing direction, is incident on the cell, a twist deformation develops, as indicated by the increased intensity detected by the detector. Typical signals obtained in the experiment are are shown in Fig. 11.

Characteristics of the signal are a finite induction time, followed by rapid and pump-intensity dependent increase in the twist which tends to saturate; this is followed by slow decay of the twist as the pump beam is turned OFF.

We note that when the pump beam is turned ON, the direct optical torque $\mathbf{D} \times \mathbf{E}$ on the director is zero; hence the twist cannot be caused by the direct optical torque. Second, we note that the surface torque density acting on the nematic to produce twist through an angle θ_t is $\sim \theta_t K/d$ where K is an elastic constant, and d is the cell thickness. The intrinsic angular momentum current density of the pump is $I\lambda/c$, where I is the intensity, so if torque to cause the twist were to originate from angular momentum transfer from the pump beam, it would require power

$$P \simeq \theta_t w_o^2 \frac{Kc}{\lambda d} \tag{5}$$

where w_o is the beam waist. Estimating $\theta_t = \pi/2$, $w_o = 1$ mm, $K = 10^{-11}$N, we obtain $P \approx 400$ mW. Experimentally, however, $P = 20$ mW; and it is clear therefore that the torque causing the twist cannot originate in angular momentum transfer from the pump beam.

We therefore consider a Brownian ratchet description of the dye dynamics.

IV Orientational Ratchet Mechanism

A salient feature of motors is that they produce motion in a system without angular momentum transfer from outside. Since in both the bulk and surface alignment experiments discussed above the liquid crystal director reorients essentially without angular momentum transfer from light, there is "rotation without torque", similar to "motion without force" in the translational ratchet schemes of Astumian [11] and Prost [12] It is possible to interpret the results of the photoalignment experiments in terms of a Brownian ratchet mechanism.

Photoexcitation and interactions between the dye and the liquid crystal host Since the observed anomalous photoalignment behavior arises due to the presence of dichroic dye molecules, it is useful to consider the photoexcitation of the dye and its interactions with the nematic host. The absorption cross-section of dichroic dye molecules is orientation dependent. In the simplest case, there is a single absorption dipole in

the dye molecule with direction $\hat{\mathbf{l}}_\mathbf{d}$, and the absorption cross-section has the form

$$\sigma = \sigma_o(\hat{\mathbf{l}}_\mathbf{d} \cdot \hat{\mathbf{E}})^2 \qquad (6)$$

where $\hat{\mathbf{E}}$ is the direction of polarization of light. After photoexcitation the dye molecule will be in an excited state with a finite lifetime, and will decay back to the ground state. Dyes such as anthraquinone[10] show such behavior. Azo-dyes are often used in photoalignment; these [34] and some others [35] undergo a trans-cis isomerization on photoexcitation. The details of this process are complicated , however, a simple two state model is sufficient to capture many of the essential features.

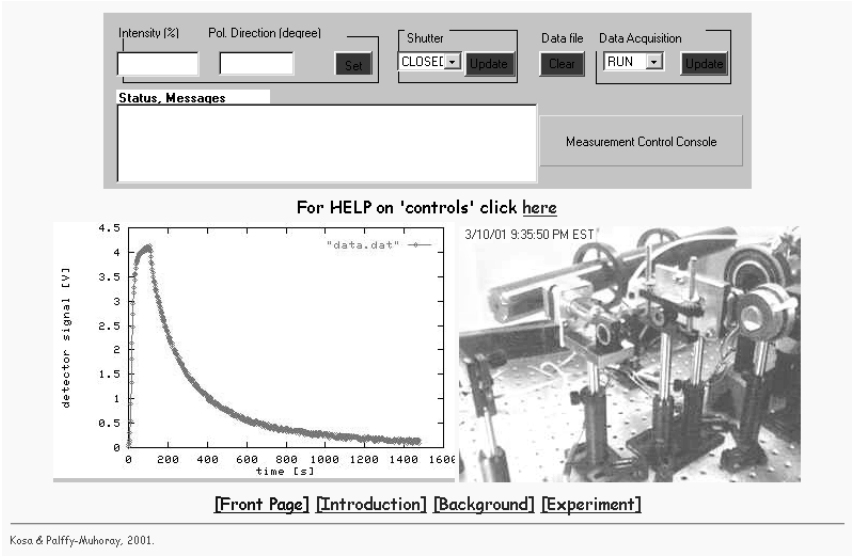

Figure 10. Typical frame form the Web-based remote photoinduced twist experiment showing the user interface, detector signal and the experimental setup.

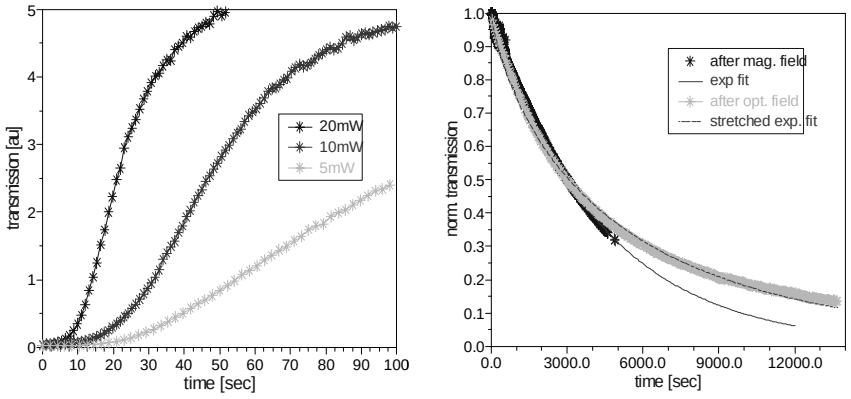

Figure 11. Intensity measured at the detector with pump ON and OFF.

The anisotropy of dichroic molecules results in anisotropic interactions with the liquid crystal host, similar to interactions between the nematic liquid crystal molecules. If symmetry axis of the molecule is along the $\hat{\mathbf{l}}_\mathbf{d}$ direction, to lowest order, the effective potential experienced by the dye in the nematic field is of the form

$$U = -U_o(\hat{\mathbf{l}}_\mathbf{d} \cdot \hat{\mathbf{n}})^2 \qquad (7)$$

where U_o is a (positive) interaction strength. A key point here is that the strength of the interaction between the liquid crystal and dye in the ground (*trans-*) state differs from that in the excited (*cis-*) state. Furthermore, the mobilities of the dye in the ground and excited states are expected to be different; this has been shown experimentally [36].

Landauer's Blowtorch: Orientational version In the original version of Landauer's blowtorch, since the temperature is shifted relative to the potential, particles near the left side of the valleys are at a higher temperature than those near the right; consequently they are more likely to be thermally excited over the potential barrier and diffuse to the left. The heat source drives a steady current of particles against an opposing viscous force; the current flows without momentum transfer from the outside. The anomalous photoalignment results can be interpreted on this basis.

In the simplest approximation, the dichroic dye molecules feel a nematic potential of the form

$$U(\theta) = -U_o \cos^2(\theta) \tag{8}$$

where θ is the angle between the nematic director $\hat{\mathbf{n}}$ and the symmetry axis $\hat{\mathbf{l}}_\mathbf{d}$ of the dye molecule. (Here it is assumed that the interaction between the liquid crystal and the dye in the ground state is the same as in the excited state.)

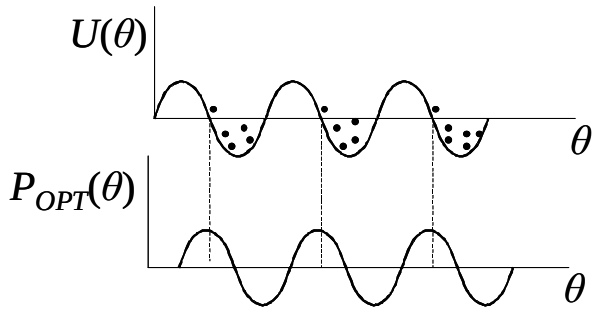

Figure 12. Landauers's Blowtorch: orientational version.

The optical power $P_{OPT}(\theta)$ absorbed by the dye per unit time from the polarized light is proportional to the cross-section, and is hence orientation dependent;

$$P_{OPT}(\theta) = -P_o \cos^2(\theta - \theta_{OPT}) \tag{9}$$

here θ_{OPT} is the angle between the polarization and the director. One may regard the photoexcitation as playing the same role as temperature. Dye molecules near the left side of the valley (that is, with absorption moments nearly parallel to the polarization of the pump beam) are more likely to be excited over the barrier and diffuse to the left (that is, rotate towards the nematic director). Light drives a steady orientational current of dye molecules against an opposing viscous torque; the current flows without momentum transfer from the outside. In the steady state, the dye exerts a steady torque on the nematic director, causing the reorientation, which is balanced by elastic torques. The dye molecules rotate steadily, the torque exerted on them by the nematic field is balanced by viscous torques.

The Flashing Ratchet: Orientational version The anomalous photoalignment results may also be interpreted [8,13] in terms of an orientational version of the the translational ratchet of Astumian [11] and Prost [12]. A schematic is shown below

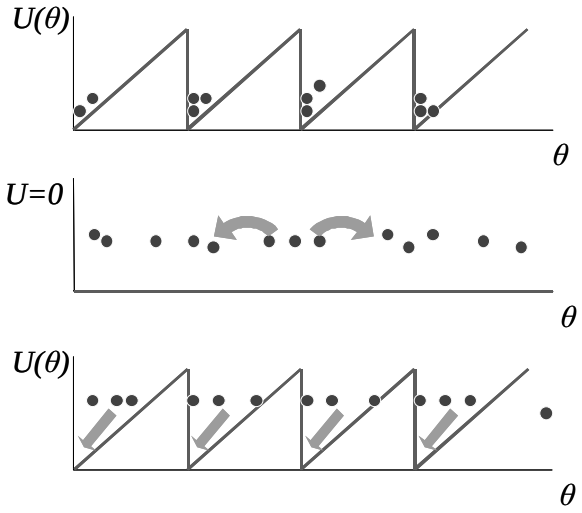

Figure 13. The orientational version of the flashing ratchet.

The dye molecules in one state (say the photoexcited state) feel the nematic potential U, and rotate towards the director. When they are in the second state (say the ground state) they no longer see the potential, and they undergo orientational diffusion. The potential is made effectively asymmetric by the orientational selectivity of the photoexcitation; dye molecules whose absorption moment is parallel to the pump polarization are preferentially excited. If the pump polarization is not orthogonal to the director, the torque on the excited dye molecules will have the same sense, resulting in a net orientational current. The potential is effectively turned off by the spontaneous decay from the excited state to the ground state.

It is worth noting that it is possible to analyze the flashing ratchet in terms of Markov processes [37].

V A Fokker-Planck Model

Dye mediated optical reorientation in the bulk The model describes the time evolution both of the director and of the dye orientational distribution. The starting point for deriving the dynamical equations

is the free energy. The energies of the excited and ground states are considered separately; the energy of the trans- isomer is

$$U_t = -U_{to}(\hat{\mathbf{l}}_\mathbf{d} \cdot \hat{\mathbf{n}})^\mathbf{2} \tag{10}$$

while for the cis- isomer it is

$$U_c = -U_{co}(\hat{\mathbf{l}}_\mathbf{d} \cdot \hat{\mathbf{n}})^\mathbf{2} \tag{11}$$

The number density of the *trans*-isomer is $\rho_t(\hat{\mathbf{l}}_\mathbf{d})$ while the number density of the *cis*-isomer is $\rho_c(\hat{\mathbf{l}}_\mathbf{d})$. The free energy of the bulk dye-liquid crystal system is

$$F = \int \{\rho_t U_t + \rho_t kT \ln \rho_t + \rho_c U_c + \rho_c kT \ln \rho_c + \frac{1}{2}K((\nabla \cdot \hat{\mathbf{n}})^\mathbf{2} + (\nabla \times \hat{\mathbf{n}})^\mathbf{2})\}\mathbf{d^3 r d\Omega} \tag{12}$$

where $d\Omega = 4\pi d^2 \hat{\mathbf{l}}_\mathbf{d}$ is the normalized element of solid angle. The chemical potential gradient drives the orientational dye current; from Eq. (12), for the *trans*-isomer, this is

$$\mathbf{J_t} = -D_\mathbf{t} \nabla_\mathbf{\Omega} \rho_\mathbf{t} - \mathbf{D_t} \rho_\mathbf{t} (\nabla_\mathbf{\Omega} \mathbf{U_t})/kT \tag{13}$$

while for the *cis*-isomer, it is

$$\mathbf{J_c} = -D_\mathbf{c} \nabla_\mathbf{\Omega} \rho_\mathbf{c} - \mathbf{D_c} \rho_\mathbf{c} (\nabla_\mathbf{\Omega} \mathbf{U_c})/kT \tag{14}$$

where ∇_Ω operates on the unit sphere. The dynamics is given by the equation of continuity, together with annihilation and creation terms due to photoexcitation. This gives, for the *trans*-isomer,

$$\frac{\partial \rho_t}{\partial t} = \nabla_\Omega \cdot [D_t \nabla_\Omega \rho_t + D_t \rho_t (\nabla_\Omega U_t)/kT] - \rho_t f_t + \rho_c f_c \tag{15}$$

and for the *cis*-isomer

$$\frac{\partial \rho_c}{\partial t} = \nabla_\Omega \cdot [D_c \nabla_\Omega \rho_c + D_c \rho_c (\nabla_\Omega U_c)/kT] - \rho_c f_c + \rho_t f_t \tag{16}$$

where

$$f_t = f_{to} e^{U_t/kT} + \nu_t (\hat{\mathbf{l}}_\mathbf{d} \cdot \hat{\mathbf{E}})^\mathbf{2} \tag{17}$$

and

$$f_c = f_{co} e^{U_c/kT} + \nu_c (\hat{\mathbf{l}}_\mathbf{d} \cdot \hat{\mathbf{E}})^\mathbf{2} \tag{18}$$

are transition rates, including photoexcitation. The director dynamics is also obtained from the free energy density $\mathcal{F}$

$$\gamma \frac{\partial \hat{\mathbf{n}}}{\partial t} = -\int \frac{\delta \mathcal{F}}{\delta \hat{\mathbf{n}}} d\Omega \tag{19}$$

where γ is the orientational viscosity and the integration is over the orientation of the dye molecules. This gives

$$\gamma \frac{\partial \hat{\mathbf{n}}}{\partial t} = \{K(\nabla^2 \hat{\mathbf{n}}) + <\rho_\mathbf{t} \nabla_\mathbf{\Omega} U_t>_\mathbf{\Omega} + <\rho_\mathbf{c} \nabla_\mathbf{\Omega} U_c>_\mathbf{\Omega}\}(\mathbf{I} - \hat{\mathbf{n}}\hat{\mathbf{n}}) \tag{20}$$

where $< >$ indicates averaging over the dye orientation; $(\mathbf{I} - \hat{\mathbf{n}}\hat{\mathbf{n}})$ is a projection operator enforcing the constraint that $\hat{\mathbf{n}}$ is a unit vector. The dye induced torque terms can be written in terms of the average orientational currents of the *trans*- and *cis*- isomers; then

$$\gamma \frac{\partial \hat{\mathbf{n}}}{\partial t} = \{K(\nabla^2 \hat{\mathbf{n}}) - \frac{kT}{D_t} <\mathbf{J_t}>_\mathbf{\Omega} - \frac{kT}{D_c} <\mathbf{J_c}>_\mathbf{\Omega}\}(\mathbf{I} - \hat{\mathbf{n}}\hat{\mathbf{n}}) \tag{21}$$

The torque on the nematic director exerted by the dye as a consequence of photoexcitation is proportional to the average orientational current of the dye. Equations (15), (16) and (20) are the coupled dynamical equations describing evolution of the orientational distribution of the dye under photexcitation in the nematic field of the liquid crystal, and optical reorientation of the bulk liquid crystal due to the dye; the direct optical torque on the liquid crystal has been ignored.

Optical alignment by dyed alignment layers The model for optical alignment at surfaces is similar to that in the bulk. The free energy of the photosensitive dye-containing alignment layer and the bulk liquid crystal is

$$F = \int (\rho_t^s U_t + \rho_t^s kT \ln \rho_t^s + \rho_c^s U_c + \rho_c^s kT \ln \rho_c^s) d\mathbf{r^2 d\Omega} + \int \frac{1}{2} \mathrm{K}((\nabla \cdot \hat{\mathbf{n}})^2 + (\nabla \times \hat{\mathbf{n}})^2)) \mathbf{d^3 r} \tag{22}$$

here ρ_t^s and ρ_c^s are the number densities per area; the first integral is over the alignment layer surface area and over the dye orientation; the second is over the bulk liquid crystal volume. The same procedure as in the previous section gives the dynamical equation for the *trans*-isomer,

$$\frac{\partial \rho_t^s}{\partial t} = \nabla_\Omega \cdot [D_t \nabla_\Omega \rho_t^s + D_t \rho_t^s (\nabla_\Omega U_t)/kT] - \rho_t^s f_t + \rho_c^s f_c \tag{23}$$

and for the *cis*-isomer

$$\frac{\partial \rho_c^s}{\partial t} = \nabla_\Omega \cdot [D_c \nabla_\Omega \rho_c^s + D_c \rho_c^s (\nabla_\Omega U_c)/kT] - \rho_c^s f_c + \rho_t^s f_t \tag{24}$$

as before. The director dynamics in the bulk, ignoring the direct optical torque, is given by the usual expression

$$\gamma \frac{\partial \hat{\mathbf{n}}}{\partial t} = K(\nabla^2 \hat{\mathbf{n}})(\mathbf{I} - \hat{\mathbf{n}}\hat{\mathbf{n}}) \tag{25}$$

however, at the photoactive surface it is given by

$$\gamma_s \frac{\partial \hat{\mathbf{n}}}{\partial t} = \{K(\hat{\mathbf{N}} \nabla \cdot \hat{\mathbf{n}} + \hat{\mathbf{N}} \times \nabla \times \hat{\mathbf{n}}) + <\rho_\mathbf{t}^\mathbf{s} \nabla_\mathbf{\Omega} U_t>_\mathbf{\Omega} + <\rho_\mathbf{c}^\mathbf{s} \nabla_\mathbf{\Omega} U_c>_\mathbf{\Omega}\}(\mathbf{I} - \hat{\mathbf{n}}\hat{\mathbf{n}}) \tag{26}$$

The torque on the nematic director at the alignment layer surface, exerted by the dye as a consequence of photoexcitation is again proportional to the average orientational current of the dye. Equations (23), (24),(25) and (26) are the coupled dynamical equations describing evolution of the orientational distribution of the dye in the alignment layer and optical reorientation of the bulk liquid crystal due to the dye; the direct optical torque on the liquid crystal has been ignored.

V.1 Computer simulations

We have solved Eqs. (23), (24), (25) and (26) numerically using simple discretization and forward time-stepping. This gives the time evolution of the orientational distribution functions $\rho_t^s(\hat{\mathbf{l}}_\mathbf{d})$ and $\rho_c^s(\hat{\mathbf{l}}_\mathbf{d})$ and the orientation of the director $\hat{\mathbf{n}}$ as a function of time. From the distribution function, the currents can be calculated. Results of simulations showing the angle of director orientation at the surface and the net current are shown below in Figs. 14 and 15.

In the simulation whose results are shown in Figs. 14 and 15, the following dimensionless parameters were used: $U_{t0} = 0.5$, $D_t = 1.0$, $U_{co} = 0.5, D_c = 0.5$, $D_{LC} = 1.0$, $f_{t0} = 0.0$, $f_{c0} = 0.5$, $\nu_t = 5.0$, $\nu_c = 0.0$, and $f_a = 50.0$. This corresponds to moderately strong interaction between the *trans*- isomer and the nematic field, but no interaction between the *cis*-isomer and the nematic; an enhanced orientational mobility of the *cis*-isomer relative to the *trans*-, a spontaneous decay of the *cis*-isomer into the *trans*-, and photoexcitation of the *trans*-isomer into the *cis*-form. By tuning these parameters, a relatively broad range of responses can be observed, but these parameters give reasonable qualitative agreement with experiment. Key features are the relatively rapid onset, after a brief induction time, of the twist deformation, resulting from photoexcitation of the dye in the alignment layer, followed by the slow decay of the twist on removing the pump excitation. It is clear from the simulation that the orientational distribution of the dye is strongly altered by the nematic field; in the absence of photoexcitation, the *trans*-isomers tend to align with the director. Photoexcitation results in orientational hole burning, that is, in depopulation of the *trans*- (and population of the *cis*-) state parallel to the pump polarization, and population of the *trans*- (and depopulation of the *cis*-) state perpendicular to the pump polarization. As the dye population undergoes this orientational redistribution, the resulting torque on the director causes it to reorient, and twist, near the photosensitive surface, towards the predominant *trans*-isomer orientation perpendicular to the polarization of the incoming pump beam. The effect of the nematic field on the dye distribution plays an important role in determining the dynamic response of the system.

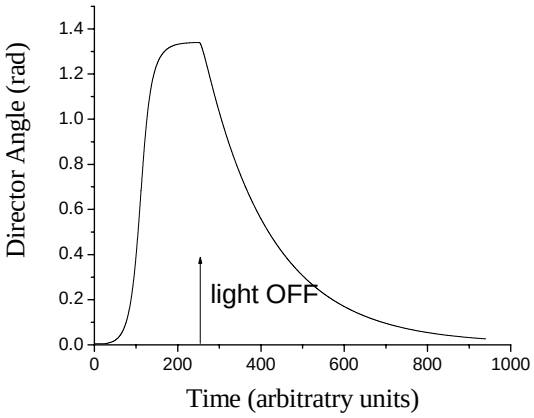

Figure 14. Simulation: director angle as function of time.

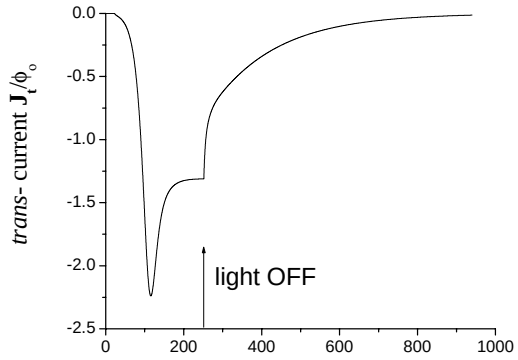

Figure 15. Simulation: average orientational *trans*-current as function of time.

A key feature of the response is that even after equilibrium is reached, while the pump is ON, there exists a steady orientational current of *trans*-isomers as can be seen in Fig. 15. (For the special case considered in this example, only the *trans*- isomer orientational current enters; in a more general case, the *cis*- current could also play a role.) The torque on the liquid crystal director $\hat{\mathbf{n}}$ is given by

$$\begin{aligned} \mathbf{\Gamma_{dye}} &= +\hat{\mathbf{n}} \times \{ < \rho_{\mathbf{t}} \nabla_{\mathbf{\Omega}} U_t >_{\mathbf{\Omega}} + < \rho_{\mathbf{c}} \nabla_{\mathbf{\Omega}} U_c >_{\mathbf{\Omega}} \} \\ &= -\hat{\mathbf{n}} \times \left\{ \frac{kT}{D_t} < \mathbf{J_t} >_{\mathbf{\Omega}} + \frac{kT}{D_c} < \mathbf{J_c} >_{\mathbf{\Omega}} \right\} \quad (27) \end{aligned}$$

Due to orientation dependent photoexcitation, the dye molecules undergo steady rotation in the nematic field, acting as rotors of a Brownian motor. This is shown schematically in Fig. 16.

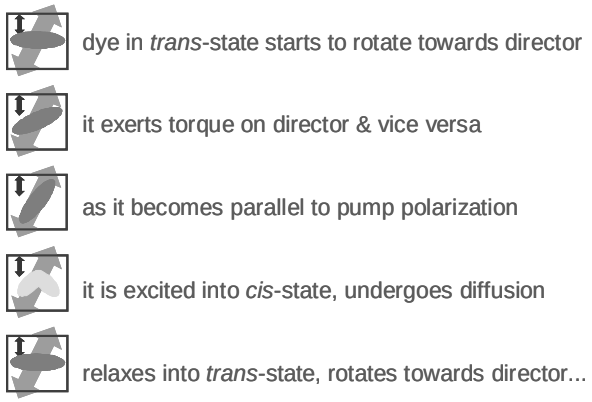

Figure 16. Schematic of the Brownian motor scenario.

The torque on the director originates in the nematic-like interaction between the liquid crystal and the dye molecules. The torque on the dye molecules can result in orientational current; in this case, viscous shear arising from the rotation carries angular momentum to the cell walls. As Eq. (3.1) shows, however, a torque may be present even if the diffusivity is zero and the dye cannot rotate, as may be the case in certain photosensitive alignment layers. In this case, angular momentum is transferred directly from the dye to the surrounding matrix.

VI Summary

Liquid crystal systems with dichroic dyes show anomalous photoalignment behavior both in the bulk and at surfaces. When irradiated by polarized light, the nematic director reorients against an elastic restoring torque essentially without the transfer of angular momentum from light to the liquid crystal. The underlying process is an orientational ratchet, with symmetric potentials, but orientation dependent transition rates. The dynamical equations are essentially the same for both bulk and surface photoalignment phenomena; in both cases, under photoexcitation, the dye molecules act as rotors of a Brownian motor. Since the director can reorient under the influence of the dye, the Fokker-Planck description of the system consists of a system of three coupled equations.

Dye-liquid crystal systems are amenable to experimental study, and can provide the opportunity for detailed comparison of experimental results and predictions of Brownian ratchet models. Insights gained in such studies would shed light on the behavior of related system, such as those in biology, and would also be useful in technological applications. These include photobuffing of substrates in liquid crystal flat panel displays, optical elements and optical memory storage.

One particularly promising area is the optomechanical response of dyed liquid crystalline gels and elastomers. Due to the strong coupling between orientational order and mechanical strain, the Brownian ratchet mechanism in these systems is expected to provide efficient conversion of light energy to mechanical work for use in applications such as light driven actuators and artificial muscles.

Acknowledgement

We acknowledge support from the NSF under ALCOM grant 89-DMR20147 and AFOSR MURI grant F49620-17-1-0014. We are indebted to B. Bergersen, who brought Landauer's blowtorch to our attention.

References

[1] A. Ashkin and J.M. Dziedzic, Phys.Rev. Lett. **30**, 139 (1973).

[2] R.A. Beth, Phys. Rev. **50**, 115, (1936).

[3] A. Saupe, in *Dynamics and Defects in Liquid Crystals*, Ed. P.E. Cladis and P. Palffy-Muhoray (Gordon & Breach, Amsterdam, 1998). The original manuscript was submitted to Phys. Rev. Lett. on July 17, (1969).

[4] B.Ya. Zel'dovich, N.F. Pilipetskii, A.V. Sukhov, and N.V. Tabiryan, JETP Lett. **31**, 264 (1980).

[5] A.S. Zolotko, V.F. Kitaeva,N. Kroo, N.N. Sobolev, and L. Csillag, JETP Lett. **32**,158 (1980).

[6] I.C. Khoo and S.L. Zhuang, Appl. Phys. Lett., **37**, 3, (1980).

[7] S.D. Durbin, S.M. Arakelian, and Y.R. Shen, Phys. Rev. Lett. **47**, 1411, (1981).

[8] P. Palffy-Muhoray and W. E, Mol. Cryst. Liq. Cryst. **320**, 193, (1998)

[9] I. Janossy, A.DD. Lloyd, and B.S. Wherret, Mol. Cryst.Liq. Cryst. **179**, 1, (990).

[10] I. Janossy, Phys. Rev. E **49**, 2957, (1994)

[11] R.D. Astumian and M. Bier, Phys.Rev.Lett.**72**, 1766, (1994).

[12] J. Prost, J.-F. Chauwin, L. Peliti, and A. Ajdari, Phys. Rev. Lett. **72**, 2652, (1994).

[13] T. Kosa, E. Weinan, and P. Palffy-Muhoray, Int. J. Eng. Sci. **38**, 1077 (2000).

[14] M. Kreuzer, L. Marrucci, D. Paparo, J. Nonlin. Opt. Phys. & Mats. **9**, 157 (2000).

[15] C.J. Pennycuick, Newton Rules Biology, (Oxford University Press, Oxford, 1992).

[16] S.M. Block, Cell, **87**,151 (1996).

[17] Y. Ishii and T. Yanagida, Single Mol. **1**, 5 (2000).

[18] Y. Okada and N. Hirokawa, Science **283**, 1152 (1999).

[19] R.D. Astumian and I. Derenyi, Biophys. J. **77**, 993 (1999).

[20] R.F. Fox and M.-H. Choi, Phys. Rev. E, **63**, 1063 (2001).

[21] P. Reimann, "Brownian Motors: noisy transport far from equilibrium", Physics Reports **361**, 57 (2002).

[22] L.M. Blinov and V.G. Chigrinov, *Electrooptic Effects in Liquid Crystals*, (Springer-Verlag, New York 1994)

[23] R. Landauer, J. Stat. Phys. **53**, 233 (1988)

[24] P. Palffy-Muhoray, in Liquid Crystals: Applications and Uses, ed. B. Bahadur (World Scientific, Singapore, 1990)

[25] A.G. Dyadyusha, T. Marusii, Y. Reznikov, A. Khiznyak, and V. Reshetnyak, JETP Lett. **56**, 17 (1992)

[26] M. Schadt, K. Schmitt, V. Kozinkov, and V. Chigrinov, Japan. J. Appl. Phys. **31**, 2155 (1992)

[27] J.L. West, X. Wang, Y. Ji, and J.R. Kelly, SID Digest **XXXVI** 703 (1995)

[28] K. Ichimura, Y. Suzuki, T. Seki, A. Hosoki, and K. Aoki, Langmuir **4**, 1214 (1988)

[29] W.M. Gibbons, P.J. Shannon, S.T. Sun, and B. Swetlin, Nature **351**, 49 (1991)

[30] W.M. Gibbons, T. Kosa, P. Palffy-Muhoray, P.J. Shannon, and S.T. Sun, Nature, **377**, 43 (1995).

[31] H. Zollinger, Color Chemistry, (VCH, Weinheim, 1991) and references therein.

[32] T. Nagele, R. Hoche, W. Zinth, J. Wachtveitl, Chem. Phys. Lett. **272**, 489 (1997).

[33] G.H. Heilmeier, L.A. Zanoni, Appl. Phys. Lett. **13**, 91 (1968).

[34] F. Weigert and M. Nakashima, Z. Phys. Chem. **34**, 258, (1929)

[35] H. Zhang, S. Shiino, A. Shishido, A. Kanazawa, O. Tsutsumi, T. Shiono, and T. Ikeda, Adv. Mater. **12**, 1336 (2000)

[36] L. Marrucci, D. Paparo, G. Abbate, E. Santamato, M. Kreuzer, P. Lehnert,, T. Vogeler, Phys. Rev. A, **58**, 4926 (1998)

[37] D. Kinderlehrer and M. Kowalczyk, Arch. for Rat. Mech. and Anal. (to appear)

[38] P. Palffy-Muhoray, T. Kosa, and E. Weinan, Mol. Cryst. Liq. Cryst. (to appear)

[39] J. Fabian and H. Hartmann, *Light Absorption of Organic Colorants* (Springer-Verlag, Berlin, 1980)